



## RESEARCH ARTICLE

10.1029/2019EA000585

## A Conceptual Framework for the Scale-Specific Stochastic Modeling of Transitions in Tropical Cyclone Intensities

## Special Section:

Nonlinear Systems in Geophysics: Past Accomplishments and Future Challenges

Saiprasanth Bhalachandran<sup>1,2</sup> , P. S. C. Rao<sup>3</sup> , and F. D. Marks Jr.<sup>4</sup> <sup>1</sup>Department of Earth, Atmospheric, and Planetary Sciences, Purdue University, West Lafayette, IN, USA, <sup>2</sup>Now at Department of Earth System Science, Stanford University, Stanford, CA, USA, <sup>3</sup>Department of Agronomy and Civil Engineering, Purdue University, West Lafayette, IN, USA, <sup>4</sup>NOAA/AOML/Hurricane Research Division, Miami, FL, USA

## Key Points:

- Multiple intensity pathways are possible for a tropical cyclone due to multiscale interactions
- We present a new approach to compute the nonstationary probabilities of tropical cyclone intensity transitions
- Novel aspects include modeling of scale-specific stochasticity and cross-scale feedbacks within a tropical cyclone

## Supporting Information:

- Supporting Information S1

## Correspondence to:

S. Bhalachandran, saipb@stanford.edu

## Citation:

Bhalachandran, S., Rao, P. S. C., & Marks Jr., F. D. (2019). A conceptual framework for the scale-specific stochastic modeling of transitions in tropical cyclone intensities. *Earth and Space Science*, 6. <https://doi.org/10.1029/2019EA000585>

Received 31 JAN 2019

Accepted 4 MAY 2019

Accepted article online 10 MAY 2019

**Abstract** At any given time, a tropical cyclone (TC) vortex has multiple intensity pathways that are possible. We conceptualize this problem as a scenario where each of the TC's intensity pathways is a distinct attractor basin, and a combination of several external and internal factors across multiple scales dictates as to which of the many pathways the TC vortex actually takes. As with any complex system, it is difficult to know the details of the multiscale processes that cause or initiate the tipping of the TC vortex into an attractor basin. A stochastic shock arising from any of the various scales within a TC vortex and the subsequent cross-scale energy transactions may rapidly increase the probability of the vortex intensifying or weakening. To address this problem and apply our conceptual framework to actual TC case studies, we formulate a novel scale-specific stochastic model that examines the multiscale energetics at and across individual wave numbers within the TC vortex. The stochastic term is modeled in a realistic manner in that the lower and higher wave numbers are treated differently. High-resolution Hurricane Weather and Research Forecast model outputs of two Bay of Bengal TCs, Phailin (intensifying) and Lehar (weakening), are used as case studies. An ensemble of intensity pathways is generated, and the nonstationary probability distributions of the intensity transitions at each time are examined. Our approach is another step toward an improved understanding of the stochastic dynamics of multiscale transitions of a TC vortex.

## 1. Problem Introduction

A number of external and internal sources and sinks serve to change the state of a tropical cyclone (TC) vortex. The state variables refer to TC characteristics such as trajectory, structure, and intensity. Unlike transitions in a TC's trajectory that is largely governed by large-scale characteristics (Marks & Shay, 1998), intensity changes in TCs are the manifestation of highly complex, nonlinear dynamical energy exchanges at and across multiple scales. As a result, transitions in TC intensities present a major challenge to the forecasters and emergency response teams. At any given time, there is a spectrum of possible intensity pathways and multiple pathways that lead to the same intensification or weakening scenarios for a TC vortex. Thus, we conceptualize the possible outcomes as nonstationary probability density functions (PDFs) of TC intensities (Figure 1). The extremes of such transitions in TC intensity are rapid intensity changes composing of rapid intensification (RI) and rapid weakening (RW)—defined as an intensity change of  $\pm 30$  knots or greater within 24 hr (Kaplan & DeMaria, 2003; Kotal & Roy Bhowmik, 2013; Wood & Ritchie, 2015). RI and RW represent the lower probability and higher impact scenarios where the multiscale feedbacks and energy exchanges within the TC vortex are distinctly different from their steady-state counterparts.

There are at least two distinct classes of scenarios through which a steady-state vortex may be pushed into any of the intensifying or weakening configurations. First, a significant change in intensity may occur within the vortex as a direct response to an abrupt external (atmospheric, oceanic, or land) forcing. Alternatively, a change in intensity may occur as a result of stochastic internal dynamics. In the first case, the vortex resilience relative to the magnitude of the external forcing determines the nature of the impact on the TC structure and intensity. Examples of such a transition are when a TC weakens in an environment with high vertical wind shear (DeMaria, 1996) or when a TC attains very high intensities in a low-sheared environment (Bhalachandran et al., 2019). Both of these scenarios are relatively easy to predict since knowledge of the large-scale environment is more or less sufficient to predict the consequent behavior of the vortex to considerably accuracy. The most difficult scenarios from a forecasting perspective are those where the external and internal dynamical forcings are of comparable strength—for example, TC vortices in moderately

©2019. The Authors.

This is an open access article under the terms of the Creative Commons Attribution-NonCommercial-NoDerivs License, which permits use and distribution in any medium, provided the original work is properly cited, the use is non-commercial and no modifications or adaptations are made.

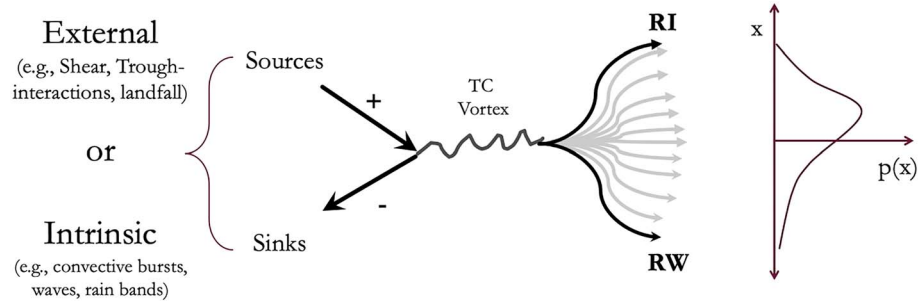


**Figure 1.** (left) Schematic indicating a change in the state (characterized by variables such as intensity) of the TC vortex as a result of multiple external or intrinsic sources and sinks acting at each time. The schematic illustrates that there are multiple pathways possible for the TC vortex. The extremes, namely, RI and RW, are also highlighted. (right) The many possible outcomes are conceptualized as nonstationary probability density functions of TC intensities ( $x$ ). TC = tropical cyclone; RI = rapid intensification; RW = rapid weakening.

sheared environments (Bhatia & Nolan, 2013; Rios-Berrios & Torn, 2017). Under such scenarios, stochastic internal dynamics may force an unexpected change in TC intensity. For example, a stochastic transition occurs as a result of a cascade of internal cross-scale interactions (provided the vortex is preconditioned in a certain manner) under the absence of any abrupt external forcing such as wind-shear or landfall. The same magnitude of external forcing can result in vastly different trajectories depending on the details of the TC's internal stochastic dynamics making such situations a forecasting nightmare.

To better understand these stochastic transitions within the TC vortex, we first view the TC as a complex, emergent system and study its dynamics subject to external and stochastic shocks. Such an approach is analogous to critical transitions and regime shifts articulated in complex system literature (Folke et al., 2010; Holling, 1973; Park et al., 2013). Studies on a wide range of complex systems (the human brain, ecosystems, financial markets, and socio-technological systems) have shed light on the importance of anticipating and adapting to regime shifts in the state of these systems even when our understanding of the details of the system behavior is limited (Beisner et al., 2003; Park & Rao, 2014; Scheffer et al., 2012). Such drastic shifts in the state of the system are of great concern from a forecasting and risk analysis perspective. For highly stochastic systems with alternative stable states (or attractor basins analogous to intensification and weakening in this study), Scheffer et al. (2012) provide a review of the various early-warning indicators or generic markers of transitions between the stable states in different complex systems. Indicators designed for complex systems cannot be used to forecast transitions in a deterministic sense. Under scenarios where deterministic solutions are not possible, the best path forward may be to create an ensemble of scenarios to compute the probabilities of intensity change at any given time. From these scenarios, we can then develop early warning indicators and resilience maps that indicate the regions that are more susceptible and regions that are resilient to such external stressors.

Generic markers of TC (rapid) intensity changes developed to date are incapable of predicting the stochastic tipping resulting from cross-scale interactions or otherwise (Bhalachandran et al., 2019). Stochastic shocks may arise from any of the scales within and external to the vortex, and our current models and diagnostics are not adept at capturing the effect of such shocks (Hendricks et al., 2010). The mere identification of thresholds or tipping points between multiple stable states may not be very useful for highly stochastic systems. In the case of such stochastic tipping, the thresholds are extremely nonstationary and emerge based on the current state of the complex system (i.e., path dependency), making the problem of anticipating significant transitions very challenging (Park, 2012; Rietkerk et al., 2004; Scheffer et al., 2009). Some progress has been made to model a TC's trajectories in response to external and stochastic forcings (Emanuel et al., 2006), but significant challenges need to be addressed before we can claim the same for TC (rapid) intensity changes. In the following section, we present a brief overview of the past efforts made toward improved TC intensity prediction from a stochastic stand point.

## 2. Strides Made Thus Far

Prior research has long recognized that given the nature of the complex system, stochasticity may arise in our model simulations due to the incorrect specifications of the initial conditions for the vortex and the environment. Lorenz, (1969, 1984) noted that a small difference in the initial condition can be amplified

over the integration time and have an impact on the mesoscale and synoptic-scale fields. In addition to the initial condition errors, uncertainty and stochasticity may arise from one of the following sources: (i) numerical formulation (especially the nonlinear terms), (ii) misrepresentation of the model physics and/or the sub-grid scale parameterizations, and (iii) inherent stochasticity in the internal dynamics (especially convection; Berner et al., 2011; Judt et al., 2016). The latter is a particularly difficult problem as a mature understanding of the stochastic nature of convection within a vortex will require a precise understanding of how individual clouds of the order of a few kilometers impact a large system like a TC, that is of the order of a few thousands of kilometers (Krishnamurti et al., 2005). Local convective processes are transient and stochastic in that not every individual localized convective event is robust enough to have an impact at a vortex scale. Nonetheless, some events aggregate and persist enough to have a system-scale response on TC characteristics.

The primary interest here is not to merely simulate every single localized convective event within a TC vortex. High-resolution three-dimensional models do capture the events at multiple scales. However, our understanding of which of these localized, transient, and stochastic events cascade to have a significant system-scale impact is still lacking. There is a critical need for a mathematical formalism to simulate the individual and aggregate vortex-scale effect of the multiscale processes and quantify the probability of episodic, stochastic transitions of a TC vortex between the many attractor basins.

Processes at different spatiotemporal scales within the vortex have different predictability limits beyond which the forecast errors are too large in a TC model simulation. Judt et al. (2016) did a Fourier decomposition of the flow field within the vortex and investigated the error growth of individual wave numbers (WNs) within TCs while imposing stochastic perturbations at various scales internal as well as external to the TC vortex. Forecast errors in the small scales (WNs  $\geq 20$ ) were found to grow rapidly and limit their predictability to around 6 to 12 hr. Medium scales (WNs 2–5) were found to have a predictability limit of 1 to 5 days, and the large scales (WNs 0 and 1), whose predictability was tied strongly to the environment, had a predictability limit of around 7 days. To account for the differences in the behavior of multiscale processes, researchers have previously used ensemble simulations of perturbed initial conditions to achieve an improved forecast as compared to individual deterministic forecasts (Berner et al., 2011; Finocchio & Majumdar, 2017; Judt & Chen, 2016; Judt et al., 2016; Tao & Zhang, 2015; Zhang & Tao, 2013). The key message here is that the different scales (WNs) ought to be treated differently due to their varied spatiotemporal characteristics as well as predictability in a model simulation.

### 3. The Way Forward

In the following sections, we introduce a scale-specific stochastic model that computes the probabilities of episodic tipping of a TC vortex between a rapidly intensifying and a rapidly weakening configurations (two attractor basins) in response to an ensemble of stochastic forcings. We start by numerically computing the energetics within a TC vortex in the spectral space (at and across individual WNs) and then add a stochastic term whose memory and amplitude are varied for individual scales. We model the stochastic shock such that it may arise from or manifest in any of the scales within the vortex and then compute the probability of such a stochastic transition at a vortex scale across an ensemble of scenarios.

#### 3.1. Data and Model Description

TCs Phailin and Lehar experienced contrasting rapid intensity changes in late 2013 and are selected as case studies here. Phailin rapidly intensified from 45 knots to 115 knots between 10 and 11 October 2013. Only 6 weeks later, Lehar reached an intensity of 75 knots, and concerns similar to Phailin were raised as the storm approached land. However, over the next 18 hr, Lehar weakened rapidly to  $\sim 30$  knots, well before landfall. The reader is referred to Bhalachandran, Nadimpalli, et al. (2019) for an in-depth analysis of these TCs.

The Hurricane Weather and Research Forecasting (HWRF) Model outputs are used in this study. HWRF is the operationally adopted, 3-D (nonaxisymmetric), near-cloud-resolving framework that allows us to disentangle and visualize the impact of the processes of interest associated with TCs (Tallapragada et al., 2014). Simulations are performed using HWRF v3.5 that has three nested domains with 27-, 9-, and 3-km grid spacing. There are 43 vertical levels, including 11 levels below 850 hPa for adequate resolution of the hurricane boundary layer. The model is nonhydrostatically mapped on a rotated latitude-longitudinal, Arakawa

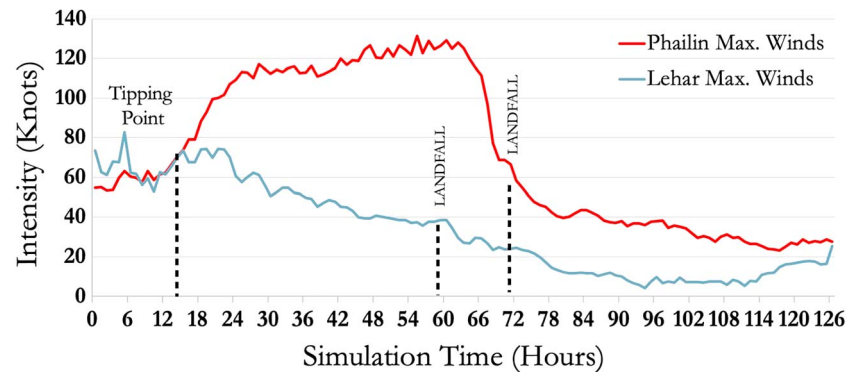


**Figure 2.** Time-series plot of intensity for Phailin initialized on 12 UTC, 9 October 2013 (red line), and Lehar initialized on 00 UTC, 26 November 2013 (blue line). The figure illustrates the contrasting rapid intensity changes between the two tropical cyclones. Highlighted are the times at which the rapid intensification and rapid weakening began and the tropical cyclones' respective landfall times.

E-staggered grid with a storm centered hybrid ( $\sigma$ -p) coordinate in the vertical direction. This model was developed by the National Centers for Environmental Prediction and the Hurricane Research Division and is annually updated. Recent updates include improved surface and microphysics schemes and a new shallow convective parameterization scheme (Mehra et al., 2018). The combination of Geophysical Fluid Dynamics Laboratory surface physics, Slab (thermal diffusion) model, a simplified Arakawa-Schubert scheme for cumulus parameterization, and Ferrier cloud microphysics along with Global Forecast System (GFS) planetary boundary layer scheme is used here. Further details can be found in Tallapragada et al. (2014). The initial and boundary conditions come from the GFS model.

The HWRP outputs for the high-resolution, inner-domain simulations are then transformed to a storm-centric, cylindrical coordinate system (using a monotonic bicubic interpolation) with a grid spacing of  $\Delta r = 1$  km and  $\Delta \theta = 1$  deg and a temporal resolution of 1 hr. We use a surface-minimum pressure centroid at each time to calculate the center of the cylindrical coordinate system. The radial extent of the transformed inner domain was 300 km.

HWRP simulations of Phailin and Lehar were performed with GFS initial conditions that captured the rapid changes in intensity (12 UTC, 9 October 2013 for Phailin, and 00 UTC, 26 November 2013 for Lehar). Figure 2 compares the HWRP simulated intensity evolutions of Phailin and Lehar. Note that due to the relatively small size of the Bay of Bengal basin, the life spans of these TCs and the time scales of their rapid intensity changes are much smaller compared to the Atlantic or Pacific hurricanes.

### 3.2. Formulation of the Stochastic Model

The aggregate kinetic energy (KE) is a better representative of vortex-scale transitions as compared to a surface-based metric of intensity (Powell & Reinhold, 2007). The aggregate KE combines the effect of the intensity and structure of the entire vortex. With this in mind, we first formulate the different types of energy pathways that can impact the KE at and across individual WNs in spectral space. This formalism is known as scale interactions (Krishnamurti et al., 2005; Saltzman, 1957). Note that it is also possible to study these multiscale energetics in the *frequency* domain where time is the dimension that is transformed. Prior studies have used the formalism of scale interactions to study the energetics between events at multiple time scales (e.g., interactions between the Madden-Julien Oscillation and other synoptic-scale events; Dubey et al., 2018; Hayashi, 1980; Krishnamurti et al., 2017).

Here high-resolution HWRP outputs of the desired storms of interest are taken, and the necessary variables are projected on to a storm-centric, cylindrical coordinate system. A Fourier transform is then performed, and the resulting azimuthal harmonics of these variables are computed within the TC vortex during periods of rapid intensity changes for the case studies of interest.

Equation (1) represents the KE of the mean flow (WN 0), and equation (2) represents the KE of WNs greater than zero, associated with azimuthal asymmetries (eddies). The complete formal equations of the above exchanges can be found in Text S1 in the supporting information.

$$\frac{\partial K_0}{\partial t} = - \sum_{n=1}^N \langle K_0 \rightarrow K_n \rangle + \langle P_0 \rightarrow K_0 \rangle - \langle K_0 \rightarrow F_0 \rangle . \quad (1)$$

$$\frac{\partial K_n}{\partial t} = \langle K_0 \rightarrow K_n \rangle + \langle K_{k,m} \rightarrow K_n \rangle + \langle P_n \rightarrow K_n \rangle - \langle K_n \rightarrow F_n \rangle . \quad (2)$$

Here the  $K_0$  and  $K_n$  represent the KE of WN 0 (mean flow) and WN  $n$ , respectively.  $K_m$  and  $K_k$  are the kinetic energies of WNs  $m$  and  $k$  that interact with WN  $n$  as a triad. Likewise,  $P_0$  and  $P_n$  represent the available potential energy (APE) of WN 0 and WN  $n$ . The terms in angular brackets indicate exchanges that are positive in the direction of the arrow. The KE of the mean flow (WN 0) could change either due to the transactions of KE with other eddy scales (known as barotropic interactions) or due to a conversion of APE to KE on the scale of the mean flow (known as baroclinic energy exchange) and frictional dissipation ( $F_0$ ). Term 1 in equation (2) represents the barotropic transfer of KE between the mean and eddies at each individual scale,  $n$ . Term 2 in equation (2) represents the nonlinear exchange of KE across different scales. Term 3 in equation (2) represents the baroclinic exchanges between APE to KE at each WN  $n$ , and the last term is the loss to friction. The generation of APE is computed as the covariance of diabatic heating and temperature, and the conversion from APE to KE is computed as the covariance of temperature and vertical velocity (see Text S1 and Krishnamurti et al., 2005, 2007).

We then rewrite the partial differential equation for KE,  $K(n, t)$ , as a first-order forward difference equation, that is,

$$K(n, t) = K(n, t - \Delta t) + \Delta t * \frac{\partial K(n, t)}{\partial t}, \quad (3)$$

where the  $K(n, t)$  and  $K(n, t - \Delta t)$  represent the KE at each scale at the current time step and the previous time step, respectively. The time step,  $\Delta t$ , is 1 hr in this case. The  $\frac{\partial K(n, t)}{\partial t}$  term is computed using the right-hand side of equations (1) and (2). Recall that this term represents the combined effect of the source and/or sink terms that act to add or subtract energy at a given scale and time. At this stage, the mean-eddy, eddy-eddy, and the APE to KE terms have been precomputed from model outputs at every time step (see Figure S1).

We now add a scale-specific stochastic forcing term  $\xi(n, t)$  to equation (3) in the following manner:

$$K(n, t) = K(n, t - \Delta t) + \Delta t * \frac{\partial K(n, t)}{\partial t} + \xi(n, t). \quad (4)$$

The questions that are yet to be addressed are the following: (i) What is the nature of the perturbations? (ii) What is the amplitude of perturbations? (iii) Does the stochastic forcing have memory or does it behave as memory-less white noise? To answer these questions, we expand the  $\xi(n, t)$  term in the following manner:

$$\xi(n, t) = \alpha(n) * \xi(n, t - \Delta t) + A(n, t) * w_t(t), \quad (5)$$

where  $\alpha(n)$  is a scale-specific memory parameter;  $A(n, t)$  is the scale-specific amplitude of the stochastic forcing; and the  $w_t(t)$  term represents a random number that is extracted from a Gaussian distribution whose mean is 0 and variance 1.0 (white noise). At each time step, the stochastic forcing is applied according to equation (5), and the  $K(n, t)$  is updated. As noted previously, the  $\frac{\partial K(n, t)}{\partial t}$  term is precomputed using the right-hand side of equations (1) and (2) and invoked at each time step.

Note that this formulation is that of a first-order auto-regressive process where the stochastic forcing depends on the value at the previous time step(s). The formulation described herein is a more sophisticated version of the stochastic KE backscatter method (cf. equation 5 of Berner et al., 2011). The novel feature of our implementation is the scale specificity in the memory (with decorrelation time,  $\tau$ ) and amplitude terms. Building-off the above-mentioned previous studies, we recognize that the asymmetries at lower WNs (WNs 0, 1 and 2 to 5) have a higher persistence in time and, therefore, are associated with some memory. On the other hand, the higher WNs (WNs > 5) are associated with no memory and are stochastic in nature. For this purpose, we write  $\alpha(n)$  as a step function which assigns a decorrelation time ( $\tau$ ) of 12 hr to WNs 0 and 1, 6 hr to WNs 2 to 5, and no memory to WNs > 5. The memory parameter,  $\alpha(n)$ , and the decorrelation time,  $\tau(n)$ , are related in the following manner:

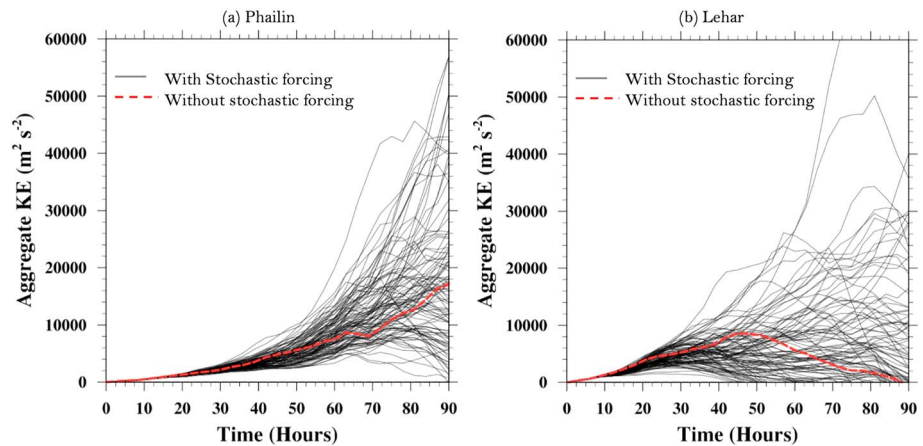


**Figure 3.** Simulations of aggregate KE (sum of KE across all wave numbers; spatially averaged through the depth of the vortex and between 0- and 300-km radii) for (a) Phailin and (b) Lehar. The gray lines represent individual realizations with the addition of stochastic forcing. The dashed red line represents the aggregate KE computed without any stochastic addition. KE = kinetic energy.

$$\alpha = \frac{\tau - 1}{\tau}. \quad (6)$$

The forcing amplitude  $A(n, t)$  is 100th of the actual amplitude of  $K(n, t)$  computed using equations (1) and (2) for each scale and time. In other words, the scale-specific forcing amplitude,  $A(n, t)$ , mimics the actual distribution of energies,  $K(n, t)$ . Since the amplitudes of the KE (or power) across the different WNs is distributed in the form of a power law (i.e., the lower WNs carry the majority of the variance), the amplitude of the stochastic term also follows suit.

A notable difference between the implementation presented herein and the stochastic KE backscatter methodology is that their stochastic perturbation was added at the *start of the forecast cycle* for each ensemble into the flow field. On the other hand, in our methodology, we have the model outputs a priori from HWRF or an equivalent model. As a result, we have the “source-sink” terms computed at each time step. The stochastic forcing is independent of the actual model run. The ensembles presented herein are diagnostic ensembles in the sense that the actual fields of the environment or vortex are not perturbed. Only the effect of such external and intrinsic fluctuations at asymmetries of various scales within the vortex is simulated herein. Once we have the modified kinetic energies for each scale and time, we invoke Parseval’s theorem to derive the aggregate KE of the vortex. Parseval’s theorem states that energy (or power) is conserved irrespective of whether we are working in physical space or Fourier space. Therefore, the system-scale KE is just the sum of the kinetic energies at individual WNs.

This procedure is iteratively repeated to create an ensemble of scenarios, and the aggregate KE evolution of the vortex is derived for each scenario. Finally, the number of transitions into either intensification or weakening configurations is computed across the ensembles, and the probability of transition to either states is presented. Note that it is not our intent to create a model that rivals or is independent of the state-of-the-art three-dimensional models currently deployed to study TC behavior. Rather, our methodology is inclusive of and dependent on their model outputs.

### 3.3. Sample Results and Discussion

Temporal evolution of the aggregated KE in Phailin and Lehar for an ensemble of 100 realizations generated by stochastic forcing are shown in Figure 3. We use the aggregate KE averaged in radius and height within the entirety of the vortex to track the vortex-scale transitions. The distribution of the realizations in Figure 3 is not bimodal, and the realizations cannot be classified into two bins such as RI or RW. The distribution of the simulated ensemble indeed resembles the PDF of TCs in the real world where RI and RW are not the only attractor basins; they merely represent the extremes among the many possibilities (cf. Figure 1).

The memory term in the stochastic forcing plays an important role in the buildup of the system-scale memory in KE leading to a positive feedback loop that may tip the vortex into a rapidly intensifying configuration. Since the amplitude of noise mimics the actual distribution of KE, when the sink terms increase (e.g., when

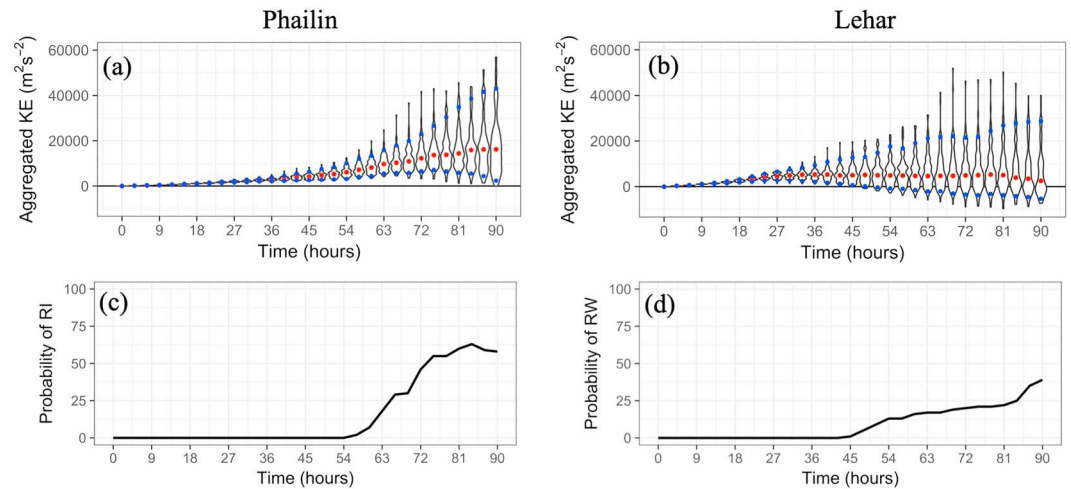


**Figure 4.** (a,b) Violin plots of the nonstationary PDFs of aggregated KE (across all ensembles) at each time for Phailin (a) and Lehar (b). The red dots indicate the median of the PDFs (50th percentile). The trajectory of the median broadly indicates the growth or decay of KE with time. The evolution of the median is analogous to the KE evolution without any stochastic forcing (cf. red dashed lines in Figure 3). Additionally, the blue dots indicate the 5th and 95th percentiles of the PDFs respectively. (c,d) The probability of RI and of RW at each time for Phailin and of RW for Lehar. Here the “RI” and “RW” are redefined as the 95th and 5th percentile of change in aggregated KE across all ensembles. KE = kinetic energy; RI = rapid intensification; RW = rapid weakening; PDF = probability density function.

the conversion from potential to KE is reduced post-landfall or due to dry-air intrusion), the noise term also reduces (negative feedback). The evolution of the two components of the noise term is shown in Figure S2. There is a large variation in the timing of the rise and fall of KE (Figures 3a and 3b) in individual realizations. Judt and Chen (2016) observed in their ensemble simulation of a rapidly intensifying TC that while the external forcing dictated the 24-hr probability of whether RI would occur or not in the first place, the intrinsic dynamics of the vortex controlled the precise timing of when the RI occurs. Our results agree with their conclusion as the variation in the stochastic forcing for the same environmental conditions results in realizations with very different timings of intensification and weakening.

An analysis of the energetics at individual WNs helps us examine which scales dominate the system-scale impact. In Phailin and Lehar, WNs 0 and 1 are seen to have a dominant impact (Figures S3 and S4). Since the KE distribution in a TC follows a power law (Krishnamurti et al., 2005, 2013), the energy content in the higher WNs (e.g., Figures S4d and S5d) are several orders of magnitude smaller than that of WN 0 or WN 1. This is not to say that the higher WNs are unimportant since the cross-scale feedbacks ensures that the signatures of the higher WNs are projected onto the lower WNs (cf. equation (2)).

The nonstationary PDFs of aggregated KE across all ensembles at each time indicate an increase in variance increases with time (as evidenced by the broadening of the PDF violins) due to the memory and feedbacks discussed above (Figures 4a and 4b). The increased variance is especially evident during the periods post the critical transitions in both Phailin and Lehar (time period after 36 hr). The ensemble coefficient of variance (Ratio of Standard Deviation to Mean at each time) is significantly higher (almost twice) during Lehar’s RW than Phailin’s RI (Figure S5). These results suggest that an increased variance and coefficient of variance might serve as early warning indicators of TC rapid intensity changes consistent with the prior literature on critical transitions in other systems (Scheffer et al., 2012).

A prerequisite to a probabilistic forecast based on this ensemble is establishing the reference thresholds. In highly stochastic systems, an idea of a fixed threshold might mislead us into drawing incorrect conclusions. These thresholds emerge from the system dynamics (Park, 2012). Let us say that we track the number of realizations that underwent a rapid increase or decrease in KE over the course of the simulation. The simulations are for KE and not intensity. Recall that RI and RW are defined as a change in intensity of at least 30 knots over 24 hr corresponding to the 95th percentile of intensity change in TCs over a long period (~30 years) in a particular basin (Kaplan et al., 2010). However, there is no equivalent definition for RI or RW in terms of energy. One way forward is to plot a PDF of the change in 24-hr KE computed between each time

$t$  and  $t + 24$  across all the realizations. Consequently, the number of realizations that underwent the 95th percentile of change in KE may be compared to the total number of realizations. Using this approach, the probability of Phailin undergoing RI and Lehar undergoing RW are plotted at each time (Figures 4c and 4d). In this manner, our framework facilitates the probabilistic forecasting of TC intensity changes based on the short-term evolution of an ensemble of trajectories.

A key point to note is that there is a difference in the timing of RI/RW predicted using intensity (Figure 2) and in the probabilities for the 95th (and 5th) percentile of the aggregate KE (Figures 4c and 4d). This suggests that the KE changes much slower than the instantaneous peak wind (intensity). This behavior is expected given that the aggregate KE is a system-scale estimate, while the intensity is based on noisy instantaneous values. Such a difference in response implores us to understand the relationship between aggregate KE and the peak wind better (Maclay et al., 2008; Powell & Reinhold, 2007). However, as we point out in section 1, the objective of this work is not to predict RI but to develop a conceptual framework that provides us with an improved understanding of the stochastic intensity transitions in TCs.

#### 4. Concluding Remarks

This article is part of a special issue titled *Nonlinear Geophysics: Past Accomplishments and Future Challenges*. Here we first review the past advances and challenges pertaining to TC rapid intensity changes, predictability, and multiscale interactions. As a step toward an improved understanding of TC intensity transitions, here we present a new conceptual framework to characterize the spectrum of possible intensity pathways for a TC vortex at any given time and quantify the nonstationary probability distributions of stochastic intensity transitions. The salient feature of this framework is the modeling of scale-specific stochasticity and cross-scale feedbacks within a TC.

Diagnostics for detecting TC (rapid) intensity changes have been developed primarily using the large-scale environmental characteristics (Kaplan & DeMaria, 2003; Kaplan et al., 2010; Rozoff et al., 2015). In a stochastic system, the same external forcing can have a variety of responses depending on the TC's internal dynamics. It is insufficient to diagnose the transitions of complex systems in a deterministic sense. Stochastic shocks will always play an important role in triggering intensity changes even in the absence of a major external event (provided the vortex is preconditioned a certain way). Recent studies have sought to vortex-scale dynamical and thermodynamical factors in addition to the large-scale variables (Bhalachandran et al., 2019; Hendricks et al., 2010). The processes within the vortex occur at multiple scales, and the challenge of segregating which of the many scales to include and which to discard remains largely unresolved.

Since it is difficult to know the details of the processes at multiple scales that may trigger or tip the vortex into one of the many attractor basins, we take an alternative approach. We examine the various energy transactions and feedbacks that occur at and across individual WNs and, importantly, how they impact the vortex at a system scale. At the core of our framework is a scale-specific stochastic model. Combining this with HWRF model outputs of case studies Phailin (intensifying) and Lehar (weakening), we compute the probabilities of episodic tipping of a TC vortex between the multiple attractor basins in response to an ensemble of stochastic forcings. A novel aspect of this study is that the memory parameter and amplitude of the stochastic term are tailored for individual scales. The stochastic shock is modeled such that it may arise from any of the scales within and external to the vortex. By modeling the stochastic term in a scale-specific manner, we show that it is possible to create ensembles that mimic the distribution of TC intensities in the real world. Further work is necessary to define the critical thresholds that can be used for the probabilistic forecasting of RI and RW specifically.

A potential caveat of this analysis is that our equations in their present form rely on a hydrostatic assumption in the vertical direction. The multiscale energetics really tell us the aggregate manifestation of organized and disorganized convection. The hydrostatic assumption is acceptable at a vortex scale since the overturning secondary circulation is in hydrostatic balance (Smith et al., 2005). However, locally, the hydrostatic assumption is bound to be violated. We seek to reformulate the equations in a nonhydrostatic sense in a follow-up study.

In summary, the conceptual framework presented here is a step toward an improved understanding and probabilistic forecasting of stochastic (rapid) intensity changes experienced by TC vortices.

**Acknowledgments**

S. B. gratefully acknowledges the financial support from NASA in the form of a NASA Earth Science Fellowship (grant NNX15AM72H). P. S. C. R. thanks the financial support from the Lee A. Rieth Distinguished Professorship Endowment. The authors appreciate the discussions with Gavan McGrath and Anamika Shreevastava and other attendees of the “Complex Systems: Synthesis for Convergence” workshop (2018). S. B. gratefully acknowledges discussions with Judith Berner regarding the SKEBS modeling framework. The authors declare no financial or nonfinancial conflict of interest regarding the work presented here. The data pertaining to this paper can be accessed online ([https://figshare.com/articles/A\\_conceptual\\_framework\\_for\\_the\\_scale-specific\\_stochastic\\_modeling\\_of\\_transitions\\_in\\_tropical\\_cyclone\\_intensities/8066240](https://figshare.com/articles/A_conceptual_framework_for_the_scale-specific_stochastic_modeling_of_transitions_in_tropical_cyclone_intensities/8066240)).

**References**

Beisner, B. E., Haydon, D. T., & Cuddington, K. (2003). Alternative stable states in ecology. *Frontiers in Ecology and the Environment*, 1(7), 376–382.

Berner, J., Ha, S.-Y., Hacker, J., Fournier, A., & Snyder, C. (2011). Model uncertainty in a mesoscale ensemble prediction system: Stochastic versus multiphysics representations. *Monthly Weather Review*, 139(6), 1972–1995.

Bhalachandran, S., Haddad, Z. S., Hristova-Velva, S. M., & Marks Jr, F. (2019). The relative importance of factors influencing tropical cyclone rapid intensity changes. *Geophysical Research Letters*, 46, 2282–2292. <https://doi.org/10.1029/2018GL079997>

Bhalachandran, S., Nadimpalli, R., Osuri, K., Marks Jr, F., Gopalakrishnan, S., Subramanian, S., et al. (2019). On the processes influencing rapid intensity changes of tropical cyclones over the Bay of Bengal. *Scientific Reports*, 9(1), 3382.

Bhatia, K. T., & Nolan, D. S. (2013). Relating the skill of tropical cyclone intensity forecasts to the synoptic environment. *Weather and Forecasting*, 28(4), 961–980.

DeMaria, M. (1996). The effect of vertical shear on tropical cyclone intensity change. *Journal of the Atmospheric Sciences*, 53(14), 2076–2088.

Dubey, S., Krishnamurti, T. N., & Kumar, V. (2018). On scale interactions between the MJO and synoptic scale. *Quarterly Journal of the Royal Meteorological Society*, 144(717), 2727–2747.

Emanuel, K., Ravela, S., Vivant, E., & Risi, C. (2006). A statistical deterministic approach to hurricane risk assessment. *Bulletin of the American Meteorological Society*, 87(3), 299–314.

Finocchio, P. M., & Majumdar, S. J. (2017). The predictability of idealized tropical cyclones in environments with time-varying vertical wind shear. *Journal of Advances in Modeling Earth Systems*, 9, 2836–2862. <https://doi.org/10.1002/2017MS001168>

Folke, C., Carpenter, S. R., Walker, B., Scheffer, M., Chapin, T., & Rockström, J. (2010). Resilience thinking: Integrating resilience, adaptability and transformability. *Ecology and society*, 15(4), 20.

Hayashi, Y. (1980). Estimation of nonlinear energy transfer spectra by the cross-spectral method. *Journal of the Atmospheric Sciences*, 37(2), 299–307.

Hendricks, E. A., Peng, M. S., Fu, B., & Li, T. (2010). Quantifying environmental control on tropical cyclone intensity change. *Monthly Weather Review*, 138(8), 3243–3271.

Holling, C. S. (1973). Resilience and stability of ecological systems. *Annual Review of Ecology and Systematics*, 4(1), 1–23.

Judt, F., & Chen, S. S. (2016). Predictability and dynamics of tropical cyclone rapid intensification deduced from high-resolution stochastic ensembles. *Monthly Weather Review*, 144(11), 4395–4420.

Judt, F., Chen, S. S., & Berner, J. (2016). Predictability of tropical cyclone intensity: Scale-dependent forecast error growth in high-resolution stochastic kinetic-energy backscatter ensembles. *Quarterly Journal of the Royal Meteorological Society*, 142(694), 43–57.

Kaplan, J., & DeMaria, M. (2003). Large-scale characteristics of rapidly intensifying tropical cyclones in the North Atlantic basin. *Weather and Forecasting*, 18(6), 1093–1108.

Kaplan, J., DeMaria, M., & Knaff, J. A. (2010). A revised tropical cyclone rapid intensification index for the Atlantic and Eastern North Pacific Basins. *Weather and Forecasting*, 25(1), 220–241.

Kotal, S., & Roy Bhowmik, S. (2013). Large-scale characteristics of rapidly intensifying tropical cyclones over the Bay of Bengal and a rapid intensification (RI) index. *Mausam*, 64(1), 13–24.

Krishnamurti, T., Dubey, S., Kumar, V., Deepa, R., & Bhardwaj, A. (2017). Scale interaction during an extreme rain event over Southeast India. *Quarterly Journal of the Royal Meteorological Society*, 143(704), 1442–1458.

Krishnamurti, T., Pattnaik, S., Stefanova, L., Kumar, T. V., Mackey, B. P., O’shay, A., & Pasch, R. J. (2005). The hurricane intensity issue. *Monthly Weather Review*, 133(7), 1886–1912.

Krishnamurti, T., Stefanova, L., & Misra, V. (2013). Scale interactions. In *Tropical meteorology* (pp. 169–196). New York, NY: Springer.

Krishnamurti, T., Stefanova, L., Watson, L., & Pattnaik, S. (2007). Addressing hurricane intensity through angular momentum and scale energetics approaches. *Pure and Applied Geophysics*, 164(8–9), 1429–1441.

Lorenz, E. N. (1969). The predictability of a flow which possesses many scales of motion. *Tellus*, 21(3), 289–307.

Lorenz, E. N. (1984). Irregularity: A fundamental property of the atmosphere. *Tellus A*, 36(2), 98–110.

Maclay, K. S., DeMaria, M., & Vonder Haar, T. H. (2008). Tropical cyclone inner-core kinetic energy evolution. *Monthly Weather Review*, 136(12), 4882–4898.

Marks, F. D., & Shay, L. K. (1998). Landfalling tropical cyclones: Forecast problems and associated research opportunities. *Bulletin of the American Meteorological Society*, 79(2), 305–323.

Mehra, A., Tallapragada, V., Zhang, Z., Liu, B., Zhu, L., Wang, W., & Kim, H.-S. (2018). Advancing the state of the art in operational tropical cyclone forecasting at NCEP. *Tropical Cyclone Research and Review*, 7(1), 51–56.

Park, J. (2012). Complex coupled engineered systems: Resilience and efficiency in design and management (Ph.D. Thesis). <https://docs.lib.purdue.edu/dissertations/AAI3556560>

Park, J., & Rao, P. S. C. (2014). Regime shifts under forcing of non-stationary attractors: Conceptual model and case studies in hydrologic systems. *Journal of Contaminant Hydrology*, 169, 112–122.

Park, J., Seager, T. P., Rao, P. S. C., Convertino, M., & Linkov, I. (2013). Integrating risk and resilience approaches to catastrophe management in engineering systems. *Risk Analysis*, 33(3), 356–367.

Powell, M. D., & Reinhold, T. A. (2007). Tropical cyclone destructive potential by integrated kinetic energy. *Bulletin of the American Meteorological Society*, 88(4), 513–526.

Rietkerk, M., Dekker, S. C., De Ruiter, P. C., & van de Koppel, J. (2004). Self-organized patchiness and catastrophic shifts in ecosystems. *Science*, 305(5692), 1926–1929.

Rios-Berrios, R., & Torn, R. D. (2017). Climatological analysis of tropical cyclone intensity changes under moderate vertical wind shear. *Monthly Weather Review*, 145(5), 1717–1738.

Rozoff, C. M., Velden, C. S., Kaplan, J., Kossin, J. P., & Wimmers, A. J. (2015). Improvements in the probabilistic prediction of tropical cyclone rapid intensification with passive microwave observations. *Weather and Forecasting*, 30(4), 1016–1038.

Saltzman, B. (1957). Equations governing the energetics of the larger scales of atmospheric turbulence in the domain of wave number. *Journal of Meteorology*, 14(6), 513–523.

Scheffer, M., Bascompte, J., Brock, W. A., Brovkin, V., Carpenter, S. R., Dakos, V., et al. (2009). Early-warning signals for critical transitions. *Nature*, 461(7260), 53.

Scheffer, M., Carpenter, S. R., Lenton, T. M., Bascompte, J., Brock, W., Dakos, V., et al. (2012). Anticipating critical transitions. *Science*, 338(6105), 344–348.

- Smith, R. K., Montgomery, M. T., & Zhu, H. (2005). Buoyancy in tropical cyclones and other rapidly rotating atmospheric vortices. *Dynamics of Atmospheres and Oceans*, *40*(3), 189–208.
- Tallapragada, V., Bernardet, L., Gopalakrishnan, S., Kwon, Y., Liu, Q., Marchok, T., et al. (2014). Hurricane Weather Research and Forecasting (HWRF) model: 2013 scientific documentation. *HWRF Development Testbed Center*. (Tech. Rep. 99). Retrieved from [https://dtcenter.org/HurrWRF/users/docs/scientific\\_documents/](https://dtcenter.org/HurrWRF/users/docs/scientific_documents/)
- Tao, D., & Zhang, F. (2015). Effects of vertical wind shear on the predictability of tropical cyclones: Practical versus intrinsic limit. *Journal of Advances in Modeling Earth Systems*, *7*, 1534–1553. <https://doi.org/10.1002/2015MS000474>
- Wood, K. M., & Ritchie, E. A. (2015). A definition for rapid weakening of North Atlantic and eastern North Pacific tropical cyclones. *Geophysical Research Letters*, *42*, 10–091. <https://doi.org/10.1002/2015GL066697>
- Zhang, F., & Tao, D. (2013). Effects of vertical wind shear on the predictability of tropical cyclones. *Journal of the Atmospheric Sciences*, *70*(3), 975–983.